Anchored and labile pools of Calcineurin are enabled by a disordered AKAP scaffold

Authors

Matthew Watson[a], Teresa Almeida[a], Arundhati Ray[a], Christina Hanack[b], Rory Elston[a], Joan Btesh[b], Peter McNaughton[c] & Katherine Stott[a,*]

[a]Department of Biochemistry, University of Cambridge, 80 Tennis Court Road, Cambridge CB2 1GA, UK

[b]Stevenage Bioscience Catalyst, Gunnels Wood Rd, Stevenage SG1 2FX

[c]Wolfson Centre for Age-Related Diseases, King's College London, Guy's Campus, London Bridge, London, SE1 1UL, UK

[*]To whom correspondence should be addressed: ks123@cam.ac.uk

Present addresses:

TA: Astex Therapeutics, 436 Cambridge Science Park, Milton Road, Cambridge, CB4 0QA, UK

AR: School of Life Sciences, Gibbet Hill Campus, The University of Warwick, Coventry CV4 7AL

CH: Axxam SpA, Via Meucci 3, 20091 Bresso (Milan, Italy)

RE: Department of Biology, University of York, Heslington, York, YO10 5DD, UK

ORCIDs:

PM: 0000-0003-1946-9610

KS: 0000-0002-4014-1188

Keywords: intrinsically disordered protein, A-kinase anchoring protein (AKAP), Calcineurin, short linear motif (SLiM), multivalency, fuzzy complex

Abstract

Signalling requires precise spatial and temporal regulation of molecular interactions, which is frequently orchestrated by disordered scaffolding proteins, such as A-kinase anchoring protein 5 (AKAP5). AKAP5 contains multiple Short Linear Motifs (SLiMs) that assemble the necessary components, including the phosphatase Calcineurin, which is anchored *via* a well-characterised PxIxIT SLiM. Here we show, using a combination of biochemical and biophysical approaches, that Calcineurin also recognises additional lower-affinity SLiMs C-terminal to the PxIxIT motif. Moreover, we demonstrate that the assembly is in reality a complex system in which AKAP SLiMs spanning a wide affinity range act cooperatively to maintain distinct pools of anchored and more loosely held enzyme, analogous to the well-understood transcription factor search complexes on DNA, and compatible with the requirement for both stable anchoring and responsive downstream signalling. We conclude that the AKAP5 C-terminus is enriched in lower-affinity/mini-SLiMs that cooperate to maintain a structurally disordered but tightly regulated signalosome.

Introduction

Many enzymes involved in signal transduction are promiscuous and act in multiple pathways. Scaffolding proteins are therefore central to signalling since, by tethering signalling components and localising them, they enhance specificity and reaction rates by effectively enhancing local concentrations, and thereby achieve strict spatial and temporal control of catalysis [1,2]. A-kinase anchoring proteins (AKAPs) are a family of ca. 14 intrinsically-disordered proteins (IDPs) that were originally characterized by their ability to scaffold Protein Kinase A (PKA) [3,4], but have since been shown to assemble multiple components into 'signalosomes' that can be targeted to specific receptors or sites [5,6]. Currently there are 14 annotated AKAPs (AKAP1 to AKAP14).

58 AKAPs are typical of many IDPs in that they interact with their partners *via*
59 Short Linear Motifs (SLiMs) [7,8]. The presence of multiple SLiMs with different
60 specificities in AKAPs enables the combinatorial assembly of a dynamic multi-protein
61 hub. Much of what we understand about disordered signalling complexes is based
62 on the structures of folded partners bound to their peptide SLiMs. The rest of the
63 IDP is either not resolved or is removed to facilitate structural studies. In many cases,
64 the regions between SLiMs are assumed to be inert linkers, simply providing a
65 length-dependent increase in the effective concentration, although predictions from
66 physical models are not always reproduced experimentally, suggesting the reality is
67 more complicated [9]. The context in which IDP(R) partner interactions take place can
68 also play an important role [10]. The flanking sequences around SLiMs, although
69 disordered even in the complex, often contribute to binding [11]. Moreover, there can
70 be complex interplay between SLiMs [7]. For example, clustering or overlapping SLiMs
71 can modulate interactions through cooperativity or competition. Further, multiple
72 low-affinity SLiMs binding a single target can cooperate in a multivalent interaction
73 to increase the binding affinity. The cooperativity can take different forms: e.g.
74 allovalency (where multiple epitopes along the ligand bind a single site on a partner
75 [12]), or 'fuzziness' (where multiple interchangeable interaction sites exist on both the
76 ligand and partner [13]).
77 Here we study the interaction of the ubiquitous phosphatase Calcineurin
78 (also known as PP2B) with the C-terminal region of the scaffolding protein AKAP5
79 (previously known as AKAP79 in humans and AKAP150 in mice). Calcineurin couples
80 changes in intracellular calcium concentration to the phosphorylation state of
81 several important substrates [14]. One example is the NFAT (Nuclear Factor of
82 Activated T cells) family of transcription factors, which are dephosphorylated by
83 Calcineurin, causing their translocation to the nucleus and stimulation of
84 transcriptional programmes [15]. Like other phosphatases, Calcineurin
85 dephosphorylates sites with little sequence similarity [16,17], and primarily recognises
86 substrates or their scaffolding proteins through the interaction with SLiMs, such as

87 the PRIEIT sequence in NFATc1 [18,19]. PRIEIT is a canonical Calcineurin recognition
88 motif obeying the consensus sequence PxIxIT, a so-called 'PxIxIT' SLiM. This
89 interaction has a 25 µM affinity, which is within the optimal window for its signalling
90 function [20]. AKAP5 also has a PxIxIT SLiM with which it engages Calcineurin, albeit
91 one with a higher affinity – PIAIIIT – that is suited to anchoring (0.4 µM), while not so
92 tight that downstream signalling is inhibited [21]. In this study, we examined the
93 AKAP5/Calcineurin interaction from the perspective of the IDP scaffold. Using
94 multiple biophysical techniques including NMR spectroscopy, we show that binding
95 is far more extensive than the PxIxIT alone and we identify additional regions that
96 interact with µM - mM affinity. We hypothesise that these additional low-affinity
97 sites help to capture and maintain the high-affinity anchored Calcineurin. Moreover,
98 they provide a separate 'labile but localised' pool of rapidly dissociating and
99 rebinding Calcineurin, which could be intercepted by proteins such as NFAT that
100 compete for Calcineurin in order to enact optimal downstream signalling.
101
102 **Results**
103 **The cAKAP5 scaffold is highly disordered and monomeric**
104 AKAP5 can loosely be divided into three regions (Fig. 1a). Here, we have chosen to
105 focus on the C-terminal region (300-427; cAKAP5), which we define as the region of
106 homology across various species (Supplementary Fig. S1) following a large insertion
107 of unknown function in the rodent orthologues. The sequence contains three known
108 SLiMs that bind either enzymes (Calcineurin [22,23] or PKA [24]) or substrates (TRPV1/4 [25–
109 27]). The enzyme-bound SLiMs adopt defined secondary structures in the complexes:
110 a β-strand in the case of Calcineurin [21] and an α-helix in the case of the docking and
111 dimerization (D/D) domain of PKA [24]. There is no structural information on the SLiM
112 reported to bind TRPV1/4 [25,26].
113 To fully understand the role of disorder in the assembly of signalling
114 complexes by scaffolding proteins, it is important to understand the level and type of
115 disorder present. The term "intrinsic disorder" [28] is used to describe all proteins that

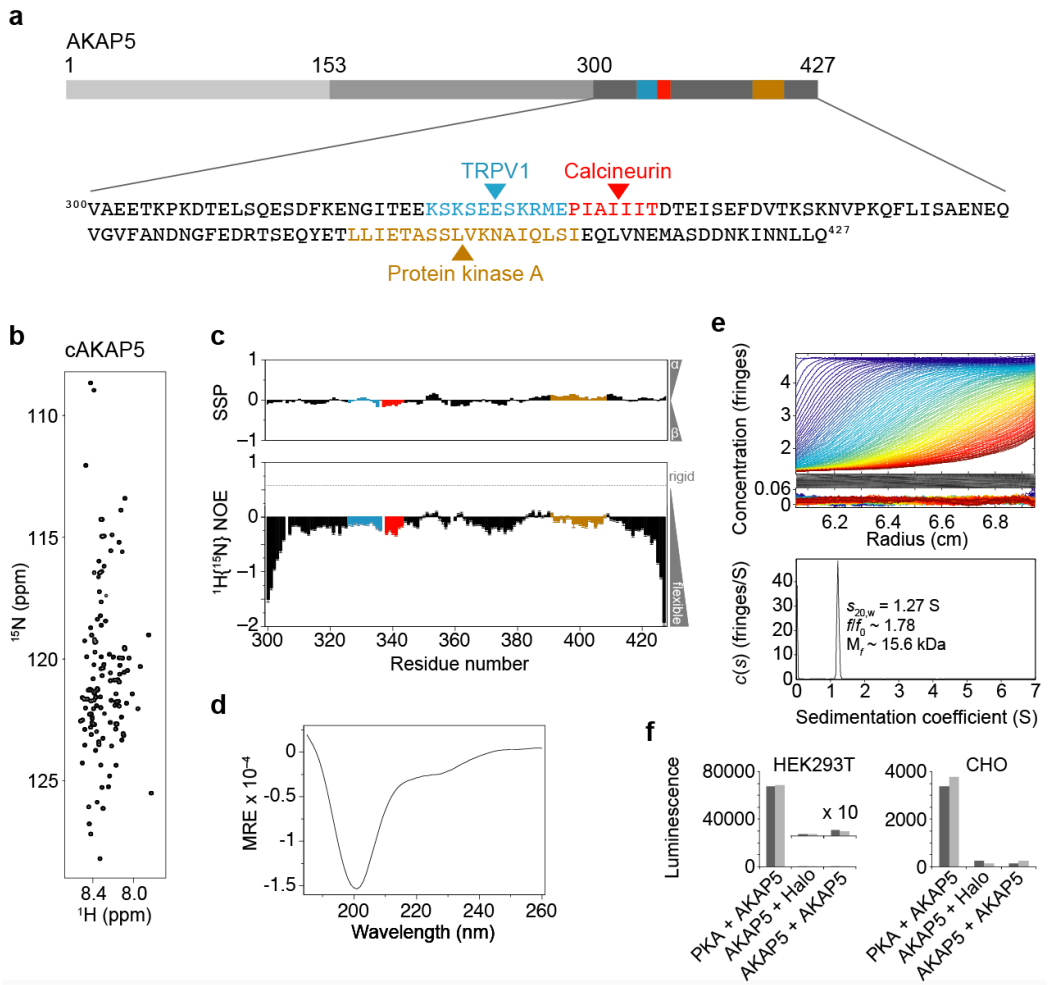

Figure 1: Structure, hydrodynamic properties and oligomeric state of AKAP5$_{300-427}$ (cAKAP5). (**a**) Schematic of AKAP5: the N-terminal region (1-152) is involved in membrane attachment; the middle region (153-299) is recognised by scaffolding proteins of the Membrane associated Guanylate Kinase family; and the C-terminal region (300-427, shown expanded) contains three known SLiMs that bind Calcineurin, PKA and substrates e.g. TRPV1. (**b**) ^{15}N HSQC of cAKAP5. (**c**) Secondary structure propensity (SSP) and Heteronuclear NOE values (colouring of SLiMs as **a**). (**d**) Far-UV CD spectrum. (**e**) Sedimentation velocity continuous *c*(*s*) distribution. (**f**) Live HEK- and CHO-cell split-luciferase assays (NanoBiT®, Promega). AKAP5 = full-length protein, PKA = regulatory PKA subunit (R2A) (positive control), Halo = HaloTag® (negative control). The order of listing indicates the orientation of the split luciferase: <protein>-LgBiT + <protein>-SmBiT.

116 populate transient structures through to those that approach true random coils (i.e.
117 those with no structural preferences and uniformly fast backbone dynamics). Two
118 spectroscopic techniques were deployed to assess and delineate regions of nascent
119 structure and to probe the backbone dynamics in cAKAP5: nuclear magnetic
120 resonance (NMR) and circular dichroism (CD). The ^{15}N-HSQC spectrum (Fig. 1b)
121 displays the low $^{1}H^{N}$ chemical-shift dispersion (0.7 ppm) and narrow line widths
122 typical of disordered proteins. A near complete assignment of the backbone H, C, N

123 and C^{β} chemical shifts was possible (Supp. Fig. S2), from which the secondary
124 structure propensity (SSP [29]) could be calculated (Fig. 1c). SSP scores in cAKAP5 are
125 close to zero with alternating stretches of weak α- or β-propensities. For
126 comparison, SSP scores are ca. +1 or –1 in stable α- and β-structures, respectively. It
127 is interesting to note that the propensities of the Calcineurin- and PKA-binding SLiMs
128 (red and yellow, respectively, in Fig. 1c) reflect the stable structures adopted in the
129 bound states (SSP_{mean} = –0.116 ± 0.038 and +0.079 ± 0.037, i.e. weak β and α,
130 respectively). Backbone dynamics were probed by $\{^{1}H\}^{15}N$ heteronuclear NOE
131 (HNOE; Fig. 1c), which reveals motions on a time-scale faster than overall tumbling
132 (HNOE < ca. +0.6). HNOEs were fairly uniform throughout cAKAP (disregarding the
133 highly mobile N- and C-termini). The average value was –0.20 ± 0.29, with no single
134 residue exhibiting a value > +0.1, and all SLiMs falling within one standard deviation
135 of the mean. This is consistent with a highly dynamic polypeptide chain. CD
136 spectroscopy also showed cAKAP5 to be predominantly disordered (Fig. 1d): the
137 signature large negative ellipticity at 200 nm was dominant, although there were
138 indications of some secondary structure (as evidenced by the weak shoulder at 222
139 nm) that is likely to be transiently populated given the results from NMR.
140 We next investigated the hydrodynamic properties of cAKAP5 by
141 sedimentation velocity analytical ultracentrifugation (SV AUC, Fig. 1e). cAKAP5
142 sedimented slowly ($s_{20,w}$ = 1.27) due to hydrodynamic friction resulting from its
143 extended nature (frictional ratio f/f_0 ~ 1.78). The fitted mass (~ 15.6 kDa) was close
144 to the calculated monomer mass (14.5 kDa). The overall picture of cAKAP5 is
145 therefore one of a highly dynamic and monomeric chain. However, there are reports
146 that AKAP5 can dimerise [30,31]. Of particular relevance to this study is the observation
147 of K333-K333 and K328-K328 intermolecular crosslinks [30], which are in the TRPV1/4
148 interaction SLiM immediately N-terminal to the Calcineurin binding site. Conversely,
149 Nygren *et al*. [32] concluded that the AKAP5/Calcineurin complex is monomeric by SEC-
150 MALS. Calcineurin is a heterodimer of A and B subunits, which are not reported to

151 oligomerise further [14], although we observed a weak propensity for further
152 dimerisation by SV AUC (Supp. Fig. S3).
153 Given AKAP5 forms complex assemblies within the cell, we investigated
154 whether full length AKAP5 dimerises in a cellular context (HEK293T and CHO) with a
155 highly sensitive live-cell luminescence assay (NanoBiT®, Promega) that uses a split-
156 luciferase reporter engineered to give reduced background. A strong
157 complementation signal was seen between PKA and AKAP5, however, AKAP5 did not
158 give a self-complementation signal in these assays that was significantly different
159 from the HaloTag® negative control (Fig. 1f). This does not preclude AKAP chains
160 being brought together *in vivo* by interactions with multimeric receptors, e.g.
161 tetrameric TRPV1 [33].
162
163 **Calcineurin binding extends beyond the PxIxIT site**
164 The Calcineurin anchoring site in cAKAP5 is at ^{337}PIAIIIT^{343}, a near-consensus PxIxIT
165 SLiM [18,19], in which ^{338}I takes the position of the consensus proline. In the crystal
166 structure, ^{337}P is not engaged and van der Waals contacts extend ca. five residues C-
167 terminal of the PxIxIT site [21]. To investigate the involvement of more distal flanking
168 regions, we titrated Calcineurin into ^{15}N-labelled cAKAP5 and followed binding by ^{15}N
169 HSQC (Fig. 2a). After one molar equivalent of Calcineurin had been added, many
170 peaks had decreased significantly in intensity, including those from residues
171 ^{338}IAIIIT^{343} (shown boxed), although the intensity loss was not complete. The changes
172 were purely to the peak intensities; no significant chemical-shift changes were seen,
173 nor did the peaks get broader, indicating that the interaction was slow on the
174 chemical-exchange timescale. No new peaks appeared, indicating slow overall
175 tumbling of the complex (Calcineurin is 80 kDa), rendering the residues in the region
176 engaging with Calcineurin invisible. The relative intensity changes when mapped
177 onto the sequence extend approx. 24 residues C-terminal beyond the PIAIIIT site,
178 with further broad dips around residues 390 and 410 (Fig. 2b). Calcineurin binding
179 thus not only extends well beyond the PIAIIIT SLiM (which could be due to weak and

transient interactions extending the footprint) but also involves distal regions of the C-terminus of cAKAP5.

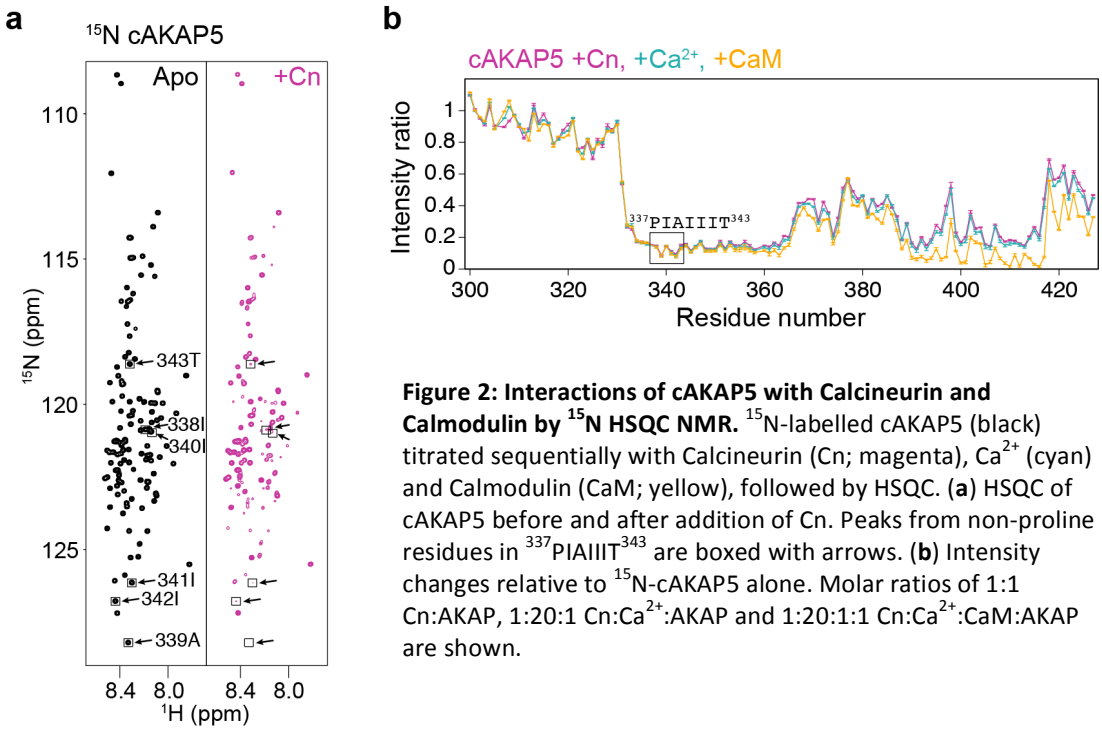

Figure 2: Interactions of cAKAP5 with Calcineurin and Calmodulin by ^{15}N HSQC NMR. ^{15}N-labelled cAKAP5 (black) titrated sequentially with Calcineurin (Cn; magenta), Ca^{2+} (cyan) and Calmodulin (CaM; yellow), followed by HSQC. (**a**) HSQC of cAKAP5 before and after addition of Cn. Peaks from non-proline residues in ^{337}PIAIIIT^{343} are boxed with arrows. (**b**) Intensity changes relative to ^{15}N-cAKAP5 alone. Molar ratios of 1:1 Cn:AKAP, 1:20:1 Cn:Ca^{2+}:AKAP and 1:20:1:1 Cn:Ca^{2+}:CaM:AKAP are shown.

Calcium and Calmodulin do not significantly alter binding

Calcineurin is activated by Ca^{2+} and Calmodulin binding [15,34]. Increases in Ca^{2+} concentration lead to partial activation of Calcineurin, through loosening association of the regulatory domain and exposure of the Calmodulin binding region. Further binding of Ca^{2+}-Calmodulin results in full activation. In addition to stimulating Calcineurin activity, this exposes a second SLiM-binding region, that interacts with πϕLxVP (π = polar, ϕ = hydrophobic) in a Ca^{2+}-Calmodulin dependent manner [35]. Although the focus of this study is primarily the dormant PxIxIT-bound 'anchored' complex, we wanted to establish whether Ca^{2+} or Ca^{2+}-Calmodulin binding alters the interaction with PIAIIIT or the new interactions found above.

We first titrated the pre-formed AKAP/Calcineurin 1:1 complex with Ca^{2+}, followed by Calmodulin. No changes were seen on addition of Ca^{2+} to a large excess (20:1; Fig. 2b). cAKAP/Calcineurin binding is therefore calcium-independent. On

197 addition of Calmodulin to 1:1:1 Calmodulin:Calcineurin:AKAP in excess Ca^{2+}, no
198 changes were seen in the region of PIAIIIT, indicating that PIAIIIT-binding of
199 Calcineurin was unaffected, in line with pull-down experiments from other
200 laboratories [30,32]. However, further peak attenuation was observed in the region C-
201 terminal but distal to the PIAIIIT site, spanning residues 390-417 (Fig. 2b). In this
202 case, peaks visibly broadened and shifted, indicating intermediate-to-fast exchange
203 on the chemical shift time scale. A separate titration of AKAP with Ca^{2+} and
204 Calmodulin but without Calcineurin present showed a similar response, but with a
205 larger mole fraction bound (Supp. Fig. S4). Calmodulin therefore appears to compete
206 with Calcineurin for binding to residues 390-417, a region ca. 50 residues from the
207 canonical PxIxIT site. This region is known to form an amphipathic helix on binding
208 PKA, and contains two clusters of bulky hydrophobic residues separated by a stretch
209 of polar residues, which is a feature of Calmodulin binding [36], although the sequence
210 was not predicted to be Calmodulin-binding by a database search (Calmodulin Target
211 Database (http://calcium.uhnres.utoron- to.ca/ctdb/)). We could not confirm
212 whether Calmodulin also bound Calcineurin in the canonical manner, but the pattern
213 of shifting and broadening of peaks continued beyond a 1:1 molar ratio of
214 Calmodulin, which is compatible with binding to two sites.
215
216 **PxIxIT is not required for binding to non-canonical sites**
217 Given the involvement of PxIxIT-flanking and distal regions of cAKAP5 in binding to
218 Calcineurin, we investigated binding to cAKAP5 in which the PIAIIIT site had been
219 deleted, $cAKAP5_{\Delta PIAIIIT}$. The titration with Calcineurin (Fig. 3a) was carried out as
220 previously. From the overlay of the intensity ratios (Fig. 3b), it is clear that the
221 immediate footprint around the PIAIIIT site (residues 330-350) is lost, as expected.
222 However, intensities more distal to the PIAIIIT site still showed significant decreases
223 in intensity, in the same regions and even more pronounced than in WT cAKAP.
224 Binding to these sites is thus PIAIIIT-independent, and competitive with PIAIIIT,
225 although it is not possible to say whether they bind the same site on the Calcineurin

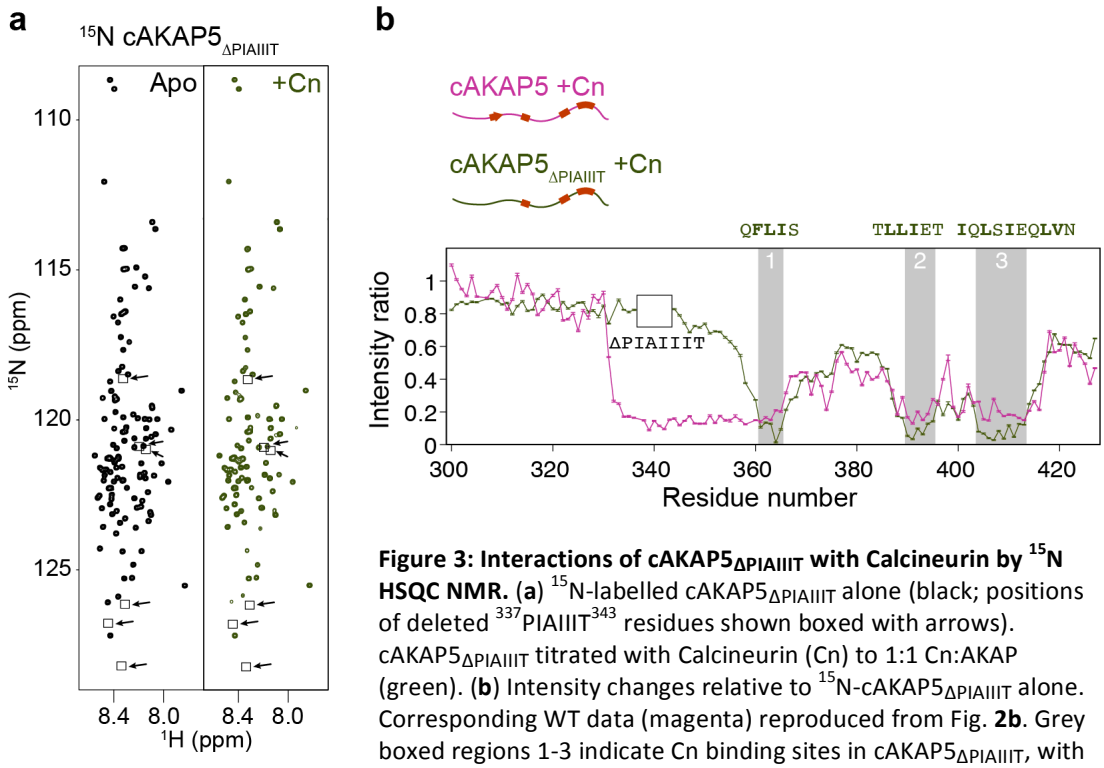

Figure 3: Interactions of cAKAP5$_{\Delta PIAIIIT}$ with Calcineurin by ^{15}N HSQC NMR. (**a**) ^{15}N-labelled cAKAP5$_{\Delta PIAIIIT}$ alone (black; positions of deleted ^{337}PIAIIIT^{343} residues shown boxed with arrows). cAKAP5$_{\Delta PIAIIIT}$ titrated with Calcineurin (Cn) to 1:1 Cn:AKAP (green). (**b**) Intensity changes relative to ^{15}N-cAKAP5$_{\Delta PIAIIIT}$ alone. Corresponding WT data (magenta) reproduced from Fig. **2b**. Grey boxed regions 1-3 indicate Cn binding sites in cAKAP5$_{\Delta PIAIIIT}$, with the corresponding amino acid sequences shown above.

side. Three regions with pronounced dips in intensity were seen, ^{361}QFLIS^{365}, ^{390}TLLIET^{395} and ^{404}IQLSIEQLVN^{413}, which we termed secondary sites 1, 2 and 3, respectively.

Inspection of the secondary site sequences revealed that they each contained three or more bulky hydrophobic residues. Given that all known Calcineurin-binding SLiMs contain hydrophobic residues [35,37], a further AKAP mutant was also tested: AKAP$_{ILVF->SA}$, in which the PIAIIIT site was present, but all the hydrophobic I, L, V and F residues in the three secondary sites were mutated to S or A to give ^{361}QASAS^{365}, ^{390}TASAET^{395} and ^{404}AQSSAEQSAN^{413}. Following reassignment of the chemical shifts, the protein was again titrated with Calcineurin (Fig. 4a). Similar to the WT, large reductions in intensities were observed in and around the PIAIIIT site (Fig. 4b). This was more pronounced in AKAP$_{ILVF->SA}$ indicating higher occupancy of the site by Calcineurin. No dips were seen at secondary sites 2 and 3, (intensities were similar to the unbound AKAP) and site 1 was partially attenuated (overlap with the PxIxIT footprint made the effect less clear). Therefore, binding of Calcineurin to the PIAIIIT or secondary sites appears to be independent but competitive, the secondary sites

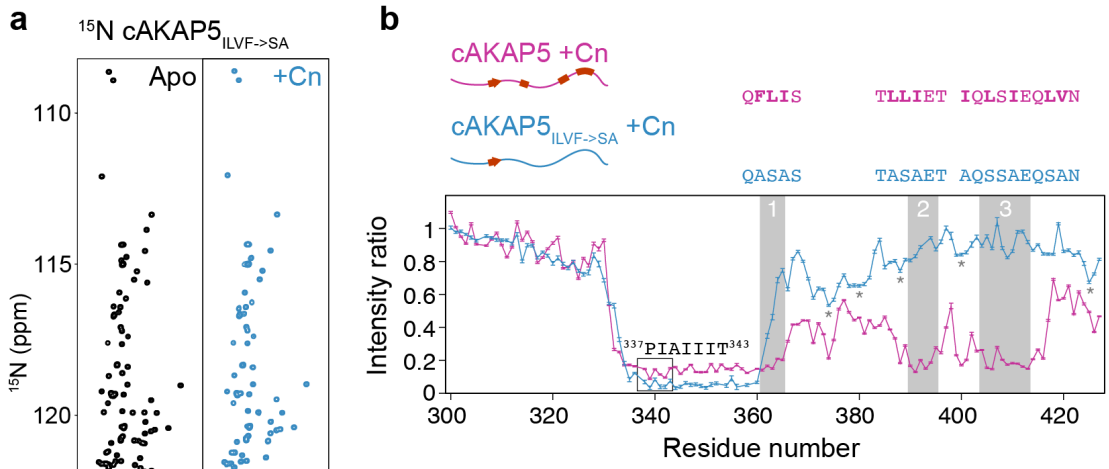

Figure 4: Interactions of cAKAP5 $_{ILVF->SA}$ with Calcineurin by ^{15}N HSQC NMR. (**a**) ^{15}N-labelled cAKAP5$_{ILVF->SA}$ alone (black). cAKAP5$_{ILVF->SA}$ titrated with Calcineurin (Cn) to 1:1 Cn:AKAP (blue). (**b**) Intensity changes relative to ^{15}N-cAKAP5$_{ILVF->SA}$ alone. Corresponding WT data (magenta) reproduced from Fig. **2b**. Grey boxed regions 1-3 indicate 'secondary' Cn binding sites identified in Fig. **3b**, with the corresponding amino acid sequences shown above. Grey asterisks indicate potential 'mini-SLiMs' (see main text).

each constituting additional hydrophobic SLiMs. One small extra region of non-PIAIIIT interaction was apparent in AKAP$_{ILVF->SA}$ in the absence of the secondary sites: ^{371}VGVFA^{375}, which contains three bulky hydrophobic residues, and there were also weaker dips corresponding to regions containing just one or two hydrophobic residues that are potential 'mini-SLiMs': ^{378}NGFED^{382}, ^{386}EQYET^{390}, ^{398}SLVKN^{402} and ^{424}NLLQ^{427} (shown by asterisks in Fig. 4b).

Non-canonical sites sequester additional Calcineurin

The detection of three secondary Calcineurin-binding SLiMs led us to speculate about their relative affinity compared to PxIxIT, and whether they can indeed bind Calcineurin independently, as suggested by the NMR data. Modified AKAP constructs, Cys-cAKAP5, Cys-cAKAP5$_{\Delta PIAIIIT}$ and Cys-cAKAP5$_{ILVF->SA}$ were chemically biotinylated for N-terminal-specific immobilisation on a streptavidin surface so that Calcineurin binding could be assessed by Surface Plasmon Resonance (SPR). Calcineurin binding to cAKAP5 (Fig. 5a) was clear but complex: the response curves (1) had no clear plateau and (2) displayed evidence of multiple binding sites with

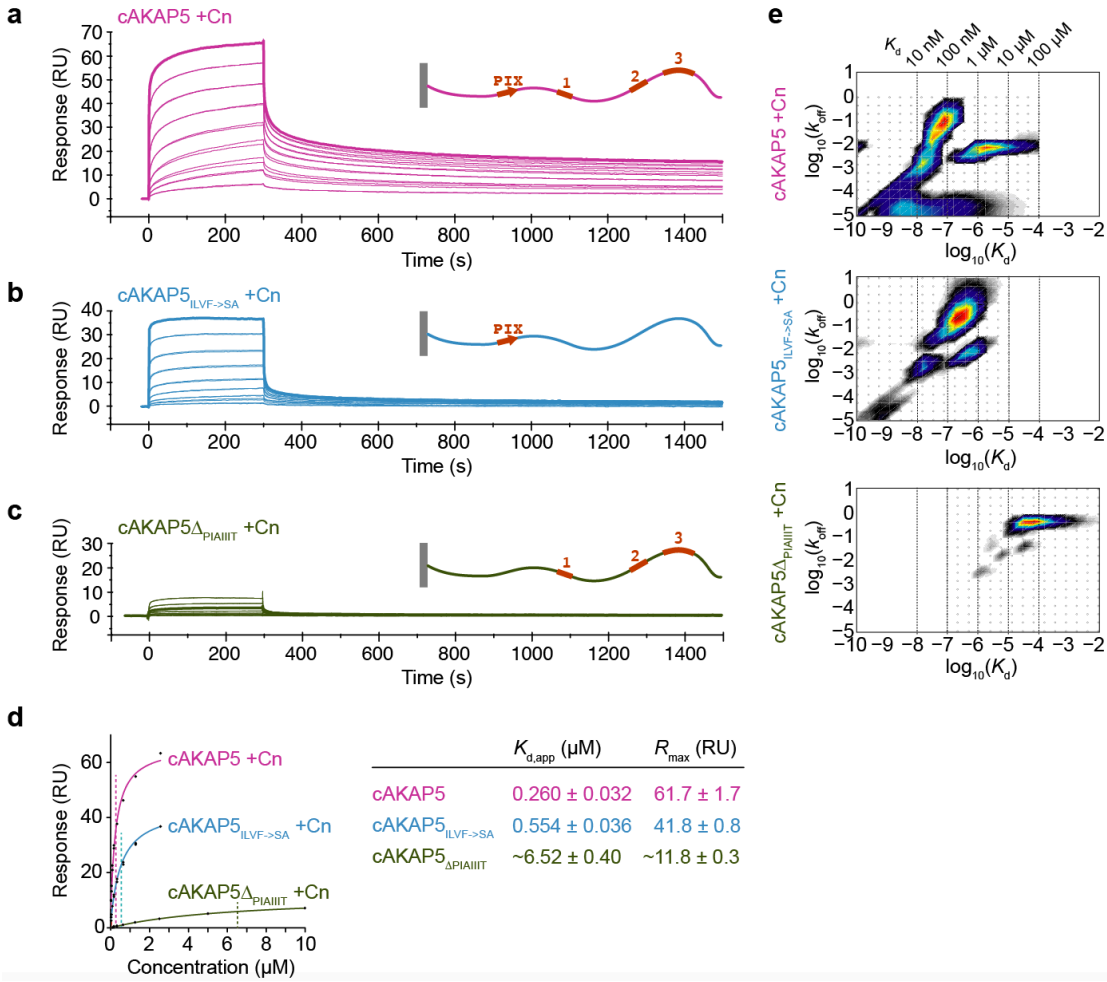

	$K_{d,app}$ (μM)	R_{max} (RU)
cAKAP5	0.260 ± 0.032	61.7 ± 1.7
cAKAP5$_{ILVF->SA}$	0.554 ± 0.036	41.8 ± 0.8
cAKAP5$_{\Delta PIAIIIT}$	~6.52 ± 0.40	~11.8 ± 0.3

Figure 5: cAKAP/Calcineurin binding by surface plasmon resonance. Calcineurin injected over a streptavidin surface pre-immobilised with (**a**) cAKAP5, (**b**) cAKAP5$_{ILVF->SA}$ or (**c**) cAKAP5$_{\Delta PIAIIIT}$. Calcineurin concentrations were 2-fold dilutions from 2.56 μM (cAKAP5 and cAKAP5$_{ILVF->SA}$) or 10 μM (cAKAP5$_{\Delta PIAIIIT}$). (**d**) Fits of 'steady-state' response vs Calcineurin concentration used to obtain estimates of $K_{d,app}$ and R_{max}. (**e**) Surface site complexity modelled in Evilfit [38]: distribution plots of k_{off} vs K_d obtained by fitting the data from **a**-**c** using a regularization and Bayesian approach (see Supp. Fig. S5 for further details).

both fast and slow kinetics in both the association and dissociation phases. In addition, a fraction of the Calcineurin remained bound at long times. The complexity was reduced somewhat in the curves for cAKAP5$_{ILVF->SA}$ (Fig. 5b), which showed a clear saturation plateau that was absent in the WT, and complete dissociation. For cAKAP5$_{\Delta PIAIIIT}$ (Fig. 5c), the curves showed a clear plateau and complete dissociation, but weaker overall binding. Also noteworthy was that the binding curves for cAKAP5$_{ILVF->SA}$ and cAKAP5$_{\Delta PIAIIIT}$ did not sum to reproduce the cAKAP binding curve, i.e. A ≠ B + C, despite their comprising separately the two kinds of binding site present in the WT. This was particularly apparent in the dissociation phase, where

267 the WT showed a sizeable fraction of Calcineurin was essentially permanently
268 bound, while no long-lasting binding of Calcineurin was observed with either mutant.
269 The binding to the PxIxIT and the secondary sites is therefore cooperative.
270 An estimate of the K_d could be obtained from fitting the signal (RU) at the
271 end of the association period *vs* Calcineurin concentration (Fig. 5d). The values
272 obtained can only be estimates for cAKAP5 and cAKAP5$_{\Delta PIAIIIT}$ due to the lack of
273 saturation ('steady-state') of the former and the lack of high-concentration data for
274 the latter. Nevertheless, the trend in apparent K_d is clear: cAKAP5 binds Calcineurin
275 about twice as tightly compared to cAKAP5$_{ILVF->SA}$, (K_d ~0.3 vs 0.6 µM) while both
276 PIAIIIT-containing AKAP constructs bind Calcineurin with at least ten-fold higher
277 affinity than cAKAP5$_{\Delta PIAIIIT}$, which has a K_d of ~ 7 µM. Estimation of the total surface
278 capacity for Calcineurin (R_{max}) is also instructive as it gives information on the
279 stoichiometry of binding under saturating conditions. From extrapolation of the
280 binding curves, it appears that cAKAP5 can accommodate ca. 50% more Calcineurin
281 than cAKAP5$_{ILVF->SA}$ (62 vs 42 RU; Fig. 5d). The secondary sites may account for this
282 'extra' 20 RU capacity, since R_{max} for cAKAP5$_{\Delta PIAIIIT}$ is (very approximately) 12 RU.
283 Multivalent ligands such as cAKAP5 are intrinsically heterogeneous, and thus
284 deviation from ideal pseudo-first order binding kinetics is not unexpected. Such
285 systems require a different analysis strategy if they are to be properly characterised.
286 A suitable alternative approach has been developed by Schuck and colleagues
287 ('Evilfit'; [38]), which uses modern regularization methods combined with a Bayesian
288 approach to add features that are essential to explain the observed data to the
289 single species model. Such features could be populations of lower-affinity or poorly
290 reversible sites. With this approach, it was possible to obtain excellent fits to the raw
291 SPR data (Supp. Fig. S5), and to extract k_{off} vs K_d distribution plots (Fig. 5e). The
292 complexity seen for Calcineurin binding to cAKAP5 was deconvolved into 3 or 4
293 classes of surface sites: one or possibly two very similar sites with K_d 10-100 nM,
294 another with K_d 1-10 µM, and a final class with a very slow k_{off} that presumably
295 accounts for the lack of full dissociation observed even at long times (i.e. poor

296 reversibility). The number of surface site classes was reduced in cAKAP5$_{ILVF->SA}$ to one
297 main site with K_d 100 nM-1 µM. The distribution was simpler again for cAKAP5$_{\Delta PIAIIIT}$
298 which displayed a single class of sites with K_d 10-100 µM. These results support a
299 picture in which cAKAP5 acts as a multivalent surface capable of binding one or more
300 molecules of Calcineurin at different sites. There are also two indications that the
301 PIAIIIT and secondary binding sites may bind cooperatively: the K_d seems to vary by
302 as much as an order of magnitude dependent on the presence or absence of the
303 other class of site, also, there appears to be a 'long-lived' (slow k_{off}) bound
304 population that is only significant when both sites are present. This latter
305 phenomenon is reminiscent of the re-capture behaviour seen for bivalent
306 antibodies, which also show anomalously slow dissociation, or ligands rebinding to
307 receptors at cell surfaces [39].
308
309 **Discussion**
310 From our experiments, it is clear that the Calcineurin binding site in cAKAP5 is far
311 more extensive than PIAIIIT, involving additional SLiMs and 'mini-SLiMs' in the C-
312 terminal region that interact with µM-mM affinity: non-consensus SLiMs containing
313 as few as three bulky hydrophobic residues appear able to bind Calcineurin with low-
314 to-mid µM affinity (cAKAP5$_{\Delta PIAIIIT}$; Fig. 5d&e), and mini-SLiMs containing only one or
315 two hydrophobic residues produce detectable binding by ^{15}N-HSQC (Fig. 4b). These
316 additional sites cooperate to increase both the effective affinity, and the binding
317 capacity of the scaffold. The effective affinity is raised through both an increase in
318 the number of productive encounters given the high density of SLiMs, and through
319 rebinding mechanisms that reduce the diffusion of Calcineurin away from the
320 scaffold since the molecule is likely to be intercepted by another binding site rather
321 than diffusing away. This latter point is borne out directly by the lack of complete
322 dissociation of Calcineurin on cAKAP5 seen by SPR (Fig. 5a). The 'labile but localised'
323 pool of rapidly dissociating and rebinding Calcineurin can presumably also be

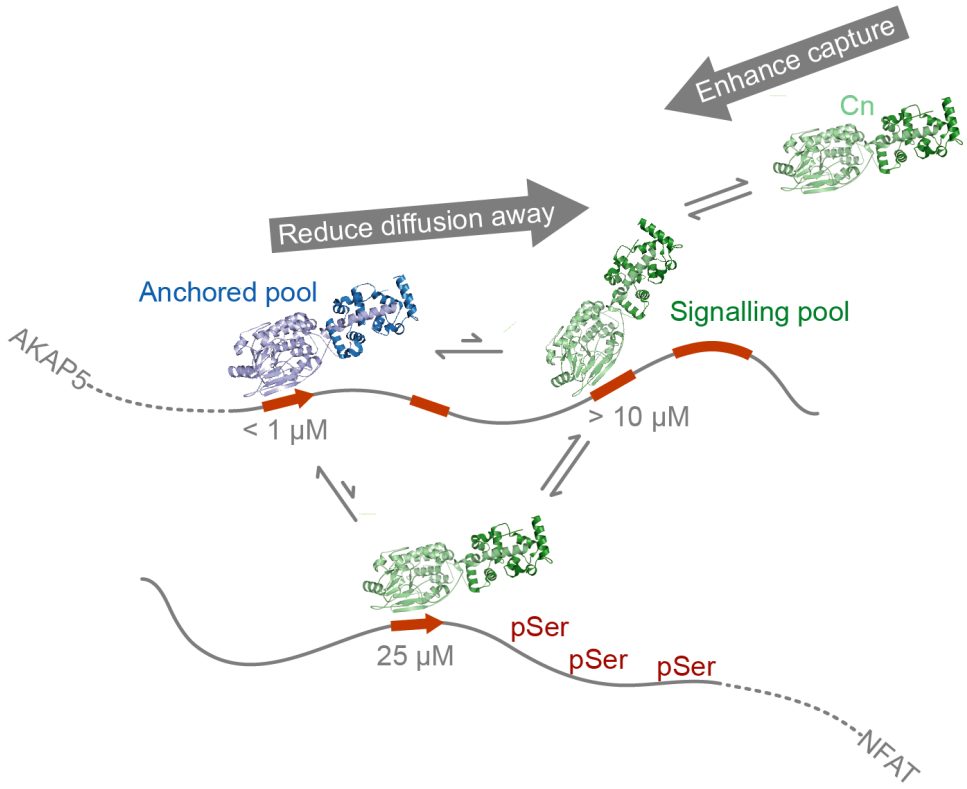

Figure 6: Non-canonical SLiMs could facilitate both anchoring and formation of a labile Calcineurin pool that enables efficient transfer to effectors. cAKAP5 captures and retains Calcineurin using its consensus PIAIIIT (red arrow) and secondary sites (red rectangles), building anchored and signalling pools of bound Calcineurin (blue and green, respectively). Calcineurin binds with lower-affinity to the secondary sites, enabling effective competition by weaker PxIxIT motifs on downstream effectors, e.g. the PRIEIT SLiM in NFAT, and optimal signalling.

324 captured by downstream effectors such as NFAT despite their mid μM affinities (Fig.
325 6).
326 These new insights are made possible by the combination of NMR mapping
327 experiments and a non-traditional approach to SPR data fitting that is validated by
328 strategic mutagenesis. The experimental study of molecular recognition by
329 disordered proteins can be very challenging due to the rapid increase in complexity
330 inherent in multivalent binding. Competition, cooperativity and multiple binding
331 modes often limit the study to global behaviour only (in which mechanistic
332 information may be lost), or dissection into simpler pairwise interactions, treating
333 the intervening sequences as inert (which may incur the loss of important
334 information on e.g. cooperativity). SPR data on such systems is often high quality in
335 both signal-to-noise and reproducibility, while being deemed “unfittable” due to the

336 ill-posed problem of decomposing a distribution of exponentials. However we find
337 that the combination of regularization and Bayesian approaches [38], designed for the
338 deconvolution of mass transport and surface heterogeneity, is also very effective at
339 decomposing multivalent interactions. The resulting distributions may be
340 subsequently validated by competition or, as we have done here, mutagenesis,
341 alongside mapping by NMR, which is both residue-specific and sensitive to a wide
342 range of interaction affinities [40].
343 In addition to the secondary sites and mini-SLiMs we establish in this study,
344 further evidence for weak, non-canonical engagement of Calcineurin with
345 hydrophobic residues is seen in the existing PxIxIT peptide/Calcineurin X-ray crystal
346 structures, in which the reverse face of the PxIxIT site provides an additional
347 potential encounter point (Supplementary Fig. 6a). In the structures, one with PVIVIT
348 [20] and one with the AKAP sequence PIAIIIT [21], the stoichiometry in the asymmetric
349 unit is two Calcineurin heterodimers to one peptide, with the second heterodimer
350 binding to the opposite side of the PxIxIT site, out of register by one residue towards
351 the C-terminus of AKAP5. The peptide thus forms an axis of pseudosymmetry. In
352 both cases, the first heterodimer that engages the consensus elements of the PxIxIT
353 sequence has a larger buried surface area and a greater number of hydrogen bonds.
354 The opposite side displays VxV or AxI, to which a second heterodimer is bound in the
355 crystal, using the same hydrophobic PxIxIT-binding groove, but with significantly
356 lower affinity, since no evidence for a 2:1 stoichiometry was seen in solution by size
357 exclusion chromatography or SEC-MALS [20,21]. However, the presence of hydrophobic
358 residues in the two 'x' positions may serve as an additional capture surface on PxIxIT,
359 even if unstable. Their presence may (partially) account for the fact that in our
360 experiments, mutation of the three distal secondary sites in $cAKAP5_{ILVF\text{->}SA}$ did not
361 restore 'pure' pseudo first-order binding characteristic of simple bimolecular
362 collisions (Fig. 5b & e). Considered as a group, PxIxIT affinities span a wide range, and
363 the fine-tuning of PxIxIT affinities by altering the 'x' positions presumably facilitates
364 evolution into either anchoring or signalling roles. It is interesting to note that during

365 selection for competitive peptide inhibitors of PxIxIT binding there was a clear
366 enrichment for hydrophobic residues (V, I and L) in the two x positions [37], while
367 many of the low affinity substrates favour charged or polar amino acids in these
368 positions that would be incompatible with the non-polar groove on Calcineurin e.g.
369 PRIEIT in NFATc1 (25 µM; Supplementary Fig. 6b).

370 Our findings also demonstrate that SLiM recognition in cAKAP5 is non-
371 exclusive: both Calcineurin and Calmodulin recognise features of the canonical PKA
372 SLiM and therefore all three are in competition for the same site (Fig. 2 & 3).
373 Interactions of one SLiM with many partners have been documented [41], and due to
374 the substitution-tolerant nature of SLiMs coupled with the conformational plasticity
375 of IDPs, may be a common feature of disordered scaffolds. In this example, PKA has a
376 higher affinity for cAKAP than Calcineurin (and presumably Calmodulin). However,
377 the *in vivo* concentration of cellular PKA is sub-µM [42] whereas concentrations of
378 Calcineurin are generally much higher (e.g. 1% of the total protein concentration in
379 brain [43]), and further concentrated at the membrane or cytoskeletal elements [44]. A
380 slowly diffusing pool of highly concentrated Calcineurin (or Calmodulin), fed by an
381 intrinsically high cellular presence and maintained by other local SLiMs, will have a
382 high effective concentration and therefore be competitive. Moreover, due to the
383 high abundance of AKAPs, there is likely to be an excess of anchoring sites compared
384 to the kinase [45].

385 Parallels can be drawn between this 'labile but localised' pool of Calcineurin
386 that supplies the canonical anchoring site with the ways transcription factors (TFs)
387 bind DNA. TFs recognize their binding site with high affinity, but also bind, albeit with
388 low affinity, to non-canonical DNA and *via* mechanisms such as sliding, jumping and
389 monkey bar strand transfer reduce the dimensionality of the search [46,47]. The
390 recognition of IDPs containing multiple SLiMs of different affinities for a partner is
391 likely to share similar properties, for which the term 'allovalency' has been coined
392 [12,48].

393 Here we uncover several Calcineurin interaction motifs spanning a range of
394 affinities from nM-mM in a short region of a scaffold protein. At least three
395 hydrophobic patches bind Calcineurin with µM affinity, which is similar to
396 Calcineurin's affinity for many of its substrates. The patches in cAKAP5 are conserved
397 across relevant AKAPs (Supplementary Fig. 1b) and do indeed appear to bestow a
398 biologically useful function: to enhance capture and anchoring, while maintaining a
399 more mobile pool of Calcineurin than would be present if the anchoring protein
400 contained one ultra-high affinity SLiM. The mM-affinity partial/mini-SLiMs may act
401 together to further conserve the hydrophobic 'capacitance' of the region responsible
402 for Calcineurin capture.
403
404 **Conclusion**
405 The scaffolding protein AKAP5 contains a well-characterised PxIxIT-motif Calcineurin
406 binding site. We characterise at least three additional binding sites of lower affinity
407 C-terminal to the PxIxIT site and propose that these additional sites create a 'labile
408 but localised' pool that both supplies Calcineurin to the canonical anchoring site and
409 to downstream effectors such as NFAT. We conclude that in AKAP5, the disordered
410 regions between anchoring SLiMs, rather than being inert tethers, are enriched in
411 lower-affinity/mini-SLiMs that act together to maintain a stable but responsive
412 signalosome.
413
414 **Materials and Methods**
415 **Constructs**
416 pcDNA™3.1 V5-His TOPO containing full length human AKAP5 with V5 and His tags
417 was obtained. $cAKAP5_{ILVF->SA}$ was generated by gene synthesis (GeneArt;
418 ThermoFisher). pOP5T was created from pOP5TT (Hyvönen *et al*., unpublished), by
419 deletion of thioredoxin leaving a TEV-removable N-terminal octa-His tag. pET15b
420 CnA CnB, which contains human PPP3CA and PPP3R1 [49] was obtained from Addgene
421 (11787). Plasmid pQE30 CaM containing rat Calmodulin (protein sequence 100%

422 identical to human) was obtained from Dermot Cooper, Department of
423 Pharmacology, University of Cambridge.
424 Cloning was carried out using standard molecular biology techniques. The
425 coding sequence for cAKAP5 was PCR amplified from pCDNA3.1 hAKAP and inserted
426 between the BamHI and HindIII sites of pHAT3 using restriction cloning. All other
427 cloning was carried out using a modified SLIC protocol based on [50]. The appropriate
428 plasmid and insert sequences (see above) with 15 bp complementary overhangs, or
429 12 bp for deletion of the PIAIIIT site were amplified using Q5 polymerase (NEB). For
430 unique Cys mutants, a Cys codon was added to the forward primer immediately after
431 the GS in the Thrombin or TEV site. Final constructs were:
432

pOP5T cAKAP5$_{ILVF->SA}$	Human AKAP 300-427 F362A, L363S, I364A, L391A, L392S, I393A, L406S, I408A, L411S, V412A with a TEV cleavable N-terminal His$_8$ tag
pOP5T Cys-cAKAP5	Human AKAP 300-427 with a TEV cleavable N-terminal His$_8$ tag and an N-terminal Cys
pOP5T Cys-cAKAP5$_{\Delta PIAIIIT}$	Human AKAP 300-427 Δ337-343 (PIAIIIT) with a TEV cleavable N-terminal His$_8$ tag and an N-terminal Cys
pOP5T Cys-cAKAP5$_{ILVF->SA}$	Human AKAP 300-427 F362A, L363S, I364A, L391A, L392S, I393A, L406S, I408A, L411S, V412A with a TEV cleavable N-terminal His$_8$ tag and an N-terminal Cys
pOP5T CaM	Rat Calmodulin with a TEV cleavable N-terminal His$_8$ tag
pBiT1.1-C AKAP5	Full-length human AKAP5-LgBiT
pBiT2.1-C AKAP5	Full-length human AKAP5-SmlBiT
NanoBiT™ Negative Control Vector	HaloTag®-SmlBiT
LgBiT-PRKAR2A Control Vector	LgBiT-PRKAR2A (RIIA regulatory subunit of PKA)

433

434 **Protein expression and purification**

435 All proteins were expressed in *E.coli* BL21(DE3) or BL21 Star (DE3) cells transformed
436 with the appropriate plasmid. For unlabelled proteins 2 L baffled flasks containing
437 500 ml of AIM LB or AIM 2YT autoinduction medium (Formedium) supplemented
438 with 50 µg/ml carbenicillin (and 1 mM $CaCl_2$ for Calmodulin) were inoculated with
439 1% starter culture in LB medium and grown overnight at 30 °C with shaking at 170
440 rpm. Labelled proteins were expressed similarly, but in M9 minimal medium
441 containing (as appropriate) 0.4 g/L ^{15}N ammonium chloride, 4g/L uniformly labelled
442 ^{13}C as the sole nitrogen and carbon sources and supplemented with 5% Celtone

443 complete medium with the appropriate isotopic labelling. Cells were grown to an
444 OD_{600} of 0.7 before induction with 0.5 mM IPTG, and grown overnight at 23 °C.
445 AKAP and Calmodulin constructs expressed from either pHAT3 or pOP5T
446 were purified as follows: cells were resuspended in IMAC buffer A (20mM Tris pH
447 8.0, 0.5 M NaCl, 10 mM imidazole) with SIGMA*FAST* EDTA free protease inhibitor
448 cocktail. Cells were lysed using an Emulsiflex and clarified lysate was incubated at 70
449 °C for 20 min. Precipitated protein was removed by centrifugation and the
450 supernatant further purified by Ni-NTA affinity chromatography. Bound proteins
451 were eluted with IMAC buffer B (A containing 400 mM imidazole) and dialysed
452 overnight into 20 mM Tris pH 8.0 using 7 kDa cut-off membrane, the His tag was
453 removed with thrombin (pHAT3) or TEV (pOP5T), uncut protein removed by passing
454 over Ni-NTA resin, and proteins further purified using a 6 ml Resource Q column
455 (Cytiva) eluted with a linear NaCl gradient 0-400 mM. DTT (2 mM) was present in all
456 steps after the initial Ni-NTA purification of proteins containing a unique cysteine.
457 Proteins were concentrated and buffer exchanged into the appropriate buffer before
458 storage at –80 °C.
459 Calcineurin was purified similarly, except that rather than heating, it was
460 precipitated from clarified lysate by addition of ammonium sulphate to 45%
461 saturation on ice before being resuspended in IMAC buffer A, and the His tag on the
462 A subunit was not removed. After concentration to ~ 5-10 mg/ml, Calcineurin was
463 further purified by size exclusion chromatography using an S200 16/600 column
464 (Cytiva) in 20 mM Tris/HCl pH 7.4, 150 mM NaCl, 2 mM DTT and stored at –80 °C.
465
466 **Protein sequences**
467
468 CAKAP5
469 GSVAEETKPKDTELSQESDFKENGITEEKSKSEESKRMEPIAIIITDTEISEFDVTKSKNVP
470 KQFLISAENEQVGVFANDNGFEDRTSEQYETLLIETASSLVKNAIQLSIEQLVNEMASDDNK
471 INNLLQ
472 ε_{205}= 420860 M^{-1} cm^{-1}
473
474 $CAKAP5_{\Delta PIAIIIT}$

GSVAEETKPKDTELSQESDFKENGITEEKSKSEESKRMEDTEISEFDVTKSKNVPKQFLISA
ENEQVGVFANDNGFEDRTSEQYETLLIETASSLVKNAIQLSIEQLVNEMASDDNKINNLLQ
ε_{205}= 401400 M^{-1} cm^{-1}

CAKAP5$_{ILVF->SA}$
GSVAEETKPKDTELSQESDFKENGITEEKSKSEESKRMEPIAIIITDTEISEFDVTKSKNVP
KQASASAENEQVGVFANDNGFEDRTSEQYETASAETASSLVKNAAQSSAEQSANEMASDDNK
INNLLQ
ε_{205}= 412260 M^{-1} cm^{-1}

Cys-CAKAP5
GSCVAEETKPKDTELSQESDFKENGITEEKSKSEESKRMEPIAIIITDTEISEFDVTKSKNV
PKQFLISAENEQVGVFANDNGFEDRTSEQYETLLIETASSLVKNAIQLSIEQLVNEMASDDN
KINNLLQ
ε_{205}= 424330 M^{-1} cm^{-1}

Cys-CAKAP5$_{\Delta PIAIIIT}$
GSVAEETKPKDTELSQESDFKENGITEEKSKSEESKRMEDTEISEFDVTKSKNVPKQFLISA
ENEQVGVFANDNGFEDRTSEQYETLLIETASSLVKNAIQLSIEQLVNEMASDDNKINNLLQ
ε_{205}= 404870 M^{-1} cm^{-1}

Cys-CAKAP5$_{ILVF->SA}$
GSVAEETKPKDTELSQESDFKENGITEEKSKSEESKRMEPIAIIITDTEISEFDVTKSKNVP
KQASASAENEQVGVFANDNGFEDRTSEQYETASAETASSLVKNAAQSSAEQSANEMASDDNK
INNLLQ
ε_{205}= 415730 M^{-1} cm^{-1}

CnA
MGSSHHHHHHSSGLVPRGSHMSEPKAIDPKLSTTDRVVKAVPFPPSHRLTAKEVFDNDGKPR
VDILKAHLMKEGRLEESVALRIITEGASILRQEKNLLDIDAPVTVCGDIHGQFFDLMKLFEV
GGSPANTRYLFLGDYVDRGYFSIECVLYLWALKILYPKTLFLLRGNHECRHLTEYFTFKQEC
KIKYSERVYDACMDAFDCLPLAALMNQQFLCVHGGLSPEINTLDDIRKLDRFKEPPAYGPMC
DILWSDPLEDFGNEKTQEHFTHNTVRGCSYFYSYPAVCEFLQHNNLLSILRAHEAQDAGYRM
YRKSQTTGFPSLITIFSAPNYLDVYNNKAAVLKYENNVMNIRQFNCSPHPYWLPNFMDVFTW
SLPFVGEKVTEMLVNVLNICSDDELGSEEDGFDGATAAARKEVIRNKIRAIGKMARVFSVLR
EESESVLTLKGLTPTGMLPSGVLSGGKQTLQSATVEAIEADEAIKGFSPQHKITSFEEAKGL
DRINERMPPRRDAMPSDANLNSINKALTSETNGTDSNGSNSSNIQ

CnB
MGNEASYPLEMCSHFDADEIKRLGKRFKKLDLDNSGSLSVEEFMSLPELQQNPLVQRVIDIF
DTDGNGEVDFKEFIEGVSQFSVKGDKEQKLRFAFRIYDMDKDGYISNGELFQVLKMMVGNNL
KDTQLQQIVDKTIINADKDGDGRISFEEFCAVVGGLDIHKKMVVDV

CnA/B
ε_{280}= 53290 M^{-1} cm^{-1}

Calmodulin
GSADQLTEEQIAEFKEAFSLFDKDGDGTITTKELGTVMRSLGQNPTEAELQDMINEVDADGN
GTIDFPEFLTMMARKMKDTDSEEEIREAFRVFDKDGNGYISAAELRHVMTNLGEKLTDEEVD
EMIREADIDGDGQVNYEEFVQMMTAK
ε_{280}= 2980 M^{-1} cm^{-1}

Extinction coefficients were calculated using

https://spin.niddk.nih.gov/clore/Software/A205.html based on Anthis & Clore, 2013

[51].

529

530 **Biotin labelling**

531 Proteins were labelled using EZ-Link™ Maleimide-PEG2-Biotin (ThermoFisher) in 10
532 mM PIPES pH 6.5, 150 mM NaCl according to the manufacturer's instructions.

533

534 **Concentration measurements**

535 Protein concentrations were determined spectophotometrically using a NanoDrop
536 One^{C} instrument (ThermoFisher) at 205 nm for the AKAP constructs (due to their low
537 ε_{280}) and 280 nm for Calcineurin and Calmodulin.

538

539 **Nuclear Magnetic Resonance**

540 NMR measurements were made on ^{15}N- or ^{13}C,^{15}N-labelled proteins (~100 µM) in 10
541 mM PIPES pH 6.5, 150 mM NaCl (NMR buffer) and 10-15% $^{2}H_2O$. Experiments were
542 recorded at 25 °C on Bruker DRX600 or 800 spectrometers. Assignments were
543 obtained using a conventional triple-resonance approach (HNCA, HN(CO)CA, HNCO,
544 HNCACB, HN(CO)CACB) alongside TOCSY-^{15}N-HSQC, NOESY-^{15}N-HSQC and
545 HNN/HN(C)N experiments [52,53]. Data were processed using AZARA (v.2.7, © 1993-
546 2021; Wayne Boucher and Department of Biochemistry, University of Cambridge).
547 Triple resonance experiments were recorded with 25% nonuniform sampling, using
548 Poisson-gap sampling [54], and reconstructed using the Cambridge CS package and the
549 CS-IHT algorithm [55]. Assignments were made using CcpNmr Analysis v. 2.4 [56].
550 Chemical shifts were referenced to 2,2-dimethyl-2-silapentane-5-sulfonic acid (DSS).
551 Heteronuclear NOE values were obtained at 600 MHz with either 4 s of ^{1}H saturation
552 using a 120° pulse train or a 4 s delay prior to the first ^{15}N pulse [57]. Complexes with
553 Calcineurin were first prepared at the defined stoichiometries in 10 mM Tris/HCl pH
554 7.4, 150 mM NaCl, 2 mM DTT and then dialysed into NMR buffer. Intensity ratios
555 were calculated using fitted peak heights in Analysis. Chemical-shift differences were
556 calculated using $\Delta\delta = [(\Delta\delta^{H})^2 + (0.15 \times \Delta\delta^{N})^2]^{1/2}$ [40].

557

558 **Far-UV Circular Dichroism Spectroscopy**

559 Experiments were performed at 0.1 mg/ml over a 185-260 nm range at 25 °C in 10
560 mM PIPES pH 6.5 and 150 mM NaF and in 1 mm path-length cuvettes. Spectra were
561 acquired using an AVIV 410 spectrometer in 1 nm wavelength steps, averaged over
562 three accumulations and baseline-corrected using buffer before smoothing, using
563 the manufacturer's software. Millidegree units were converted to mean residue
564 ellipticity (MRE) with units deg cm^2 $dmol^{-1}$ res^{-1} using MRE = millideg. / {(no. residues
565 – 1) × c × *l* × 10}, where c = molar concentration and *l* = path length in cm.

566

567 **Analytical Ultracentrifugation**

568 Sedimentation velocity was measured in an Optima XL-I centrifuge (Beckman
569 Coulter). For cAKAP, standard 12 mm double-sector Epon centrepieces with sapphire
570 windows contained 400 µl of cAKAP5 at 1 mg/mL or buffer (10 mM sodium
571 phosphate pH 6.5, 150 mM NaCl). Interference data were acquired at 40 krpm using
572 an An60 Ti four-hole rotor, at 20 °C. A multi-component sedimentation coefficient
573 *c*(*s*) distribution was obtained from 100 scans collected over 22 h by direct boundary
574 modelling of the Lamm equation using Sedfit v.15 [58]. The density and viscosity of the
575 buffer (ρ = 1.0055 g/ml; η = 1.01881 cP) and the partial specific volume of the
576 protein (0.72918 ml/g) were calculated using Sednterp [59]. For Calcineurin, 12 mm
577 double-sector Epon centrepieces with sapphire windows contained 400 µl of
578 Calcineurin at 0.4 mg/mL or buffer (10 mM PIPES pH 6.5, 150 mM NaCl, 5 mM DTT).
579 Interference data were acquired at 50 krpm using an An50 Ti eight-hole rotor, at 20
580 °C. A multi-component sedimentation coefficient *c*(*s*) distribution was obtained from
581 20 scans collected over 5 h by Sedfit, as above. The density and viscosity of the
582 buffer (ρ = 1.0054 g/ml; η = 1.02631 cP) and the partial specific volume of the
583 protein (0.73431 ml/g) were calculated by Sednterp, as above.

584

585 **Cell culture**

586 HEK293T cells were cultured in 10 cm tissue culture treated dishes grown at 37 °C in
587 a 5% CO_2 atmosphere in HEPES buffered DMEM/F12 1:1 (Merck) supplemented with
588 10% fetal bovine serum and 2 mM L-glutamine. Cells were maintained in logarithmic
589 growth phase and passaged upon reaching ~80% confluence (every 2-3 days).
590
591 **Split-Luciferase Reporter Assays (NanoBiT)**
592 Split luciferase reporter assays were carried out using the Promega NanoBiT system.
593 Briefly, cells were diluted in in HEPES buffered DMEM/F12 1:1 (Merck)
594 supplemented with 10% fetal bovine serum and 2 mM L-glutamine to 50,000
595 cells/ml and plated at a density of 5000 cells per well (100 µl) in 96-well white clear-
596 bottom tissue culture treated plates (Corning 3610). Cells were grown for 24 h
597 before transfection. Cells were transiently transfected with 50 ng each of the
598 appropriate plasmids using FuGENE HD (Promega) at a FuGENE DNA ratio of 3:1.
599 After transfection cells were grown for a further 24 h before assay.
600 Plates were left to equilibrate at room temperature for 20 minutes before addition
601 of NanoGlo live cell substrate (Promega) according to the manufacturer's
602 instructions. After mixing at 800 rpm for 10 s, luminescence was assayed in a
603 PHERAstar microplate reader (BMG LABTECH) at 25 °C using bottom optics and an
604 averaging time of 10 s.
605
606 **Surface Plasmon Resonance**
607 Experiments were performed on a Biacore T200 instrument (GE) at 25 °C. Biotin-Cys-
608 cAKAP5, Biotin-Cys-cAKAP5$_{ILVF->SA}$ and Biotin-Cys-cAKAP5$_{\Delta PIAIIIT}$ were immobilised on
609 separate channels of an SA sensor chip (Cytiva). In order to optimise the analyte
610 response signal-to-noise ratio, 12 RU were immobilised for cAKAP5 and cAKAP5$_{ILVF-}$
611 $_{>SA}$, and 55 RU for cAKAP5$_{\Delta PIAIIIT}$; analyte responses for cAKAP5$_{\Delta PIAIIIT}$ were
612 subsequently re-scaled by a factor of 12/55 for comparative purposes. Binding to
613 cAKAP5 and cAKAP5$_{ILVF->SA}$ was determined in 10 mM PIPES pH 6.5, 150 mM NaCl,
614 0.05% v/v Tween20, at ten Calcineurin concentrations (0, 10, 20, 40, 80, 160, 320,

615 640, 1280 and 2560 nM). Binding to cAKAP5$_{\Delta PIAIIIT}$ was determined at nine
616 Calcineurin concentrations (0, 78, 156, 313, 625, 1250, 2500, 5000 and 10000 nM).
617 All concentrations were run in duplicate. The contact time, dissociation time and
618 flow rate were 300 s, 1200 s and 30 µL min^{-1}, respectively. The chip surface was
619 regenerated with 50 mM NaOH, 1 M NaCl for 1 or 2 x 60 s. Data were processed
620 using the manufacturer's BIAevaluation software and further analysis was carried
621 out in EVILFIT [38].
622
623 **Data availability**
624 Chemical-shift assignments for cAKAP5 (see also Supp. Fig. S2) have been deposited
625 in the BMRB with accession number XXXX.
626
627 **Acknowledgements**
628 We thank Peter Schuck, Marko Hyvönen and Anna Git for helpful discussions, the
629 NMR and Biophysics Facilities in the Department of Biochemistry, University of
630 Cambridge for access to instrumentation, and Dermot Cooper for the Calmodulin
631 plasmid. This work was supported by the Biotechnology and Biological Sciences
632 Research Council (BB/N022181/1).
633
634 **References**
635 1. Scott, J. D. & Pawson, T. Cell signaling in space and time: Where proteins come
636 together and when they're apart. *Science* **326,** 1220–1224 (2009).
637 2. Pan, C. Q., Sudol, M., Sheetz, M. & Low, B. C. Modularity and functional
638 plasticity of scaffold proteins as p(l)acemakers in cell signaling. *Cell. Signal.* **24,**
639 2143–2165 (2012).
640 3. Theurkauf, W. E. & Vallee, R. B. Molecular characterization of the cAMP-
641 dependent protein kinase bound to microtubule-associated protein 2. *J. Biol.*
642 *Chem.* **257,** 3284–3290 (1982).
643 4. Lohmann, S. M., DeCamilli, P., Einig, I. & Walter, U. High-affinity binding of the
644 regulatory subunit (R(II)) of cAMP-dependent protein kinase to microtubule-
645 associated and other cellular proteins. *Proc. Natl. Acad. Sci. U. S. A.* **81,** 6723–
646 6727 (1984).
647 5. Wong, W. & Scott, J. D. AKAP signalling complexes: Focal points in space and
648 time. *Nat. Rev. Mol. Cell Biol.* **5,** 959–970 (2004).

649 6. Torres-Quesada, O., Mayrhofer, J. E. & Stefan, E. The many faces of
650 compartmentalized PKA signalosomes. *Cell. Signal.* **37,** 1–11 (2017).
651 7. Davey, N. E., Van Roey, K., Weatheritt, R. J., Toedt, G., Uyar, B., Altenberg, B.,
652 Budd, A., Diella, F., Dinkel, H. & Gibson, T. J. Attributes of short linear motifs.
653 *Mol. Biosyst.* **8,** 268–281 (2012).
654 8. Roey, K. Van, Uyar, B., Weatheritt, R. J., Dinkel, H., Seiler, M., Budd, A., Gibson,
655 T. J. & Davey, N. E. Short linear motifs: ubiquitous and functionally diverse
656 protein interaction modules directing cell regulation. *Chem. Rev.* **114,** 6733–
657 6778 (2014).
658 9. Charlotte, S. S., Jendroszek, A. & Kjaergaard, M. Linker dependence of avidity
659 in multivalent interactions between disordered proteins. *J. Mol. Biol.* **431,**
660 4784–4795 (2019).
661 10. Bugge, K., Brakti, I., Fernandes, C. B., Dreier, J. E., Lundsgaard, J. E., Olsen, J.
662 G., Skriver, K. & Kragelund, B. B. Interactions by disorder – a matter of context.
663 *Front. Mol. Biosci.* **7,** 1–16 (2020).
664 11. Liu, B. A., Jablonowski, K., Shah, E. E., Engelmann, B. W., Jones, R. B. & Nash, P.
665 D. SH2 domains recognize contextual peptide sequence information to
666 determine selectivity. *Mol. Cell. Proteomics* **9,** 2391–2404 (2010).
667 12. Klein, P., Pawson, T. & Tyers, M. Mathematical modeling suggests cooperative
668 interactions between a disordered polyvalent ligand and a single receptor site.
669 *Curr. Biol.* **13,** 1669–1678 (2003).
670 13. Tompa, P. & Fuxreiter, M. Fuzzy complexes: polymorphism and structural
671 disorder in protein-protein interactions. *Trends Biochem. Sci.* **33,** 2–8 (2008).
672 14. Creamer, T. P. Calcineurin. *Cell Commun. Signal.* **18,** 1–12 (2020).
673 15. Li, H., Rao, A. & Hogan, P. G. Interaction of calcineurin with substrates and
674 targeting proteins. *Trends Cell Biol.* **21,** 91–103 (2011).
675 16. Donella-Deana, A., Krinks, M. H., Ruzzene, M., Klee, C. & Pinna, L. A.
676 Dephosphorylation of phosphopeptides by calcineurin (protein phosphatase
677 2B). *Eur. J. Biochem.* **219,** 109–117 (1994).
678 17. Li, X., Wilmanns, M., Thornton, J. & Köhn, M. Elucidating human phosphatase-
679 substrate networks. *Sci. Signal.* **6,** 1–15 (2013).
680 18. Aramburu, J., Garcia-Cozar, F., Raghavan, A., Okamura, H., Rao, A. & Hogan, P.
681 G. Selective inhibition of NFAT activation by a peptide spanning the
682 calcineurin targeting site of NFAT. *Mol. Cell* **1,** 627–637 (1998).
683 19. Garcia-Cozar, F. J., Okamura, H., Aramburu, J. F., Shaw, K. T. Y., Pelletier, L.,
684 Showalter, R., Villafranca, E. & Rao, A. Two-site interaction of nuclear factor of
685 activated T cells with activated calcineurin. *J. Biol. Chem.* **273,** 23877–23883
686 (1998).
687 20. Li, H., Zhang, L., Rao, A., Harrison, S. C. & Hogan, P. G. Structure of Calcineurin
688 in Complex with PVIVIT Peptide: Portrait of a Low-affinity Signalling
689 Interaction. *J. Mol. Biol.* **369,** 1296–1306 (2007).
690 21. Li, H., Pink, M. D., Murphy, J. G., Stein, A., Dell'Acqua, M. L. & Hogan, P. G.
691 Balanced interactions of calcineurin with AKAP79 regulate Ca2+-calcineurin-
692 NFAT signaling. *Nat Struct Mol Biol* **19,** 337–345 (2012).
693 22. Dell'Acqua, M. L., Dodge, K. L., Tavalin, S. J. & Scott, J. D. Mapping the protein
694 phosphatase-2B anchoring site on AKAP79. Binding and inhibition of
695 phosphatase activity are mediated by residues 315-360. *J. Biol. Chem.* **277,**

696 48796–48802 (2002).
697 23. Oliveria, S. F., Dell'Acqua, M. L. & Sather, W. A. AKAP79/150 anchoring of
698 calcineurin controls neuronal L-Type Ca2+ channel activity and nuclear
699 signaling. *Neuron* **55,** 261–275 (2007).
700 24. Newlon, M. G., Roy, M., Morikis, D., Carr, D. W., Westphal, R., Scott, J. D. &
701 Jennings, P. A. A novel mechanism of PKA anchoring revealed by solution
702 structures of anchoring complexes. *EMBO J.* **20,** 1651–1662 (2001).
703 25. Btesh, J., Fischer, M. J., Stott, K. & McNaughton, P. A. Mapping the binding site
704 of TRPV1 on AKAP79: implications for inflammatory hyperalgesia. *J. Neurosci.*
705 **33,** 9184–9193 (2013).
706 26. Mack, K. & Fischer, M. J. M. Disrupting sensitization of TRPV4. *Neuroscience*
707 **352,** 1–8 (2017).
708 27. Zhang, X., Li, L. & McNaughton, P. A. Proinflammatory mediators modulate
709 the heat-activated ion channel TRPV1 via the scaffolding protein AKAP79/150.
710 *Neuron* **59,** 450–461 (2008).
711 28. Dunker, A. K., Babu, M. M., Barbar, E., Blackledge, M., Bondos, E., Dosztányi,
712 Z., Dyson, H. J., Forman-kay, J., Gsponer, J., Han, K., Jones, D. T., Longhi, S.,
713 Metallo, S. J., Nishikawa, K., Nussinov, R., Obradovic, Z., Pappu, V., Rost, B.,
714 Selenko, P., Subramaniam, V., Joel, L., Tompa, P., Uversky, V. N., Dunker, A. K.,
715 Babu, M. M., Barbar, E., Blackledge, M., Sarah, E., Dosztányi, Z., Dyson, H. J.,
716 Forman-kay, J., Fuxreiter, M., Gsponer, J., Han, K., Jones, D. T., Longhi, S.,
717 Metallo, S. J., Nishikawa, K., Nussinov, R., Obradovic, Z., Pappu, R. V, Rost, B.,
718 Selenko, P., Subramaniam, V., Joel, L., Dunker, A. K., Babu, M. M., Barbar, E.,
719 Blackledge, M., Bondos, S. E., Dosztányi, Z., Jane, H., Forman-kay, J., Fuxreiter,
720 M., Gsponer, J., Han, K., Jones, D. T., Longhi, S. & Steven, J. What's in a name?
721 Why these proteins are intrinsically disordered. *Intrinsically Disord. Proteins* **1,**
722 1–5 (2013).
723 29. Marsh, J. A., Singh, V. K., Jia, Z. & Forman-Kay, J. D. Sensitivity of secondary
724 structure propensities to sequence differences between α- and γ-synuclein:
725 Implications for fibrillation. *Protein Sci.* **15,** 2795–2804 (2006).
726 30. Gold, M. G., Stengel, F., Nygren, P. J., Weisbrod, C. R., Bruce, J. E., Robinson, C.
727 V, Barford, D. & Scott, J. D. Architecture and dynamics of an A-kinase
728 anchoring protein 79 (AKAP79) signaling complex. *Proc. Natl. Acad. Sci. U. S. A.*
729 **108,** 6426–6431 (2011).
730 31. Patel, N., Stengel, F., Aebersold, R. & Gold, M. G. Molecular basis of AKAP79
731 regulation by calmodulin. *Nat. Commun.* **8,** (2017).
732 32. Nygren, P. J., Mehta, S., Schweppe, D. K., Langeberg, L. K., Whiting, J. L.,
733 Weisbrod, C. R., Bruce, J. E., Zhang, J., Veesler, D. & Scott, J. D. Intrinsic
734 disorder within AKAP79 fine-tunes anchored phosphatase activity toward
735 substrates and drug sensitivity. *Elife* **6,** 1–25 (2017).
736 33. Liao, M., Cao, E., Julius, D. & Cheng, Y. Structure of the TRPV1 ion channel
737 determined by electron cryo-microscopy. *Nature* **504,** 107–12 (2013).
738 34. Rumi-Masante, J., Rusinga, F. I., Lester, T. E., Dunlap, T. B., Williams, T. D.,
739 Dunker, A. K., Weis, D. D. & Creamer, T. P. Structural basis for activation of
740 calcineurin by calmodulin. *J. Mol. Biol.* **415,** 307–317 (2012).
741 35. Sheftic, S. R., Page, R. & Peti, W. Investigating the human Calcineurin
742 Interaction Network using the πϕLxVP SLiM. *Sci. Rep.* **6,** 1–11 (2016).

743 36. Tidow, H. & Nissen, P. Structural diversity of calmodulin binding to its target
744 sites. *FEBS J.* **280,** 5551–5565 (2013).
745 37. Aramburu, J., Yaffe, M. B., López-Rodríguez, C., Cantley, L. C., Hogan, P. G. &
746 Rao, A. Affinity-driven peptide selection of an NFAT inhibitor more selective
747 than cyclosporin A. *Science* **285,** 2129–2133 (1999).
748 38. Schuck, P. & Zhao, H. The role of mass transport limitation and surface
749 heterogeneity in the biophysical characterization of macromolecular binding
750 processes by SPR biosensing. *Methods Mol. Biol.* **627,** 15–54 (2010).
751 39. Lagerholm, B. C. & Thompson, N. L. Theory for ligand rebinding at cell
752 membrane surfaces. *Biophys. J.* **74,** 1215–1228 (1998).
753 40. Zuiderweg, E. Mapping protein–protein interactions in solution by NMR
754 spectroscopy. *Biochemistry* **41,** (2002).
755 41. Hsu, W. L., Oldfield, C. J., Xue, B., Meng, J., Huang, F., Romero, P., Uversky, V.
756 N. & Dunker, A. K. Exploring the binding diversity of intrinsically disordered
757 proteins involved in one-to-many binding. *Protein Sci.* **22,** 258–273 (2013).
758 42. Beavo, J. A., Bechtel, P. J. & Krebs, E. G. Activation of protein kinase by
759 physiological concentrations of cyclic AMP. *Proc. Natl. Acad. Sci. U. S. A.* **71,**
760 3580–3583 (1974).
761 43. Yakel, J. L. Calcineurin regulation of synaptic function: From ion channels to
762 transmitter release and gene transcription. *Trends Pharmacol. Sci.* **18,** 124–
763 134 (1997).
764 44. Shibasaki, F., Hallin, U. & Uchino, H. Calcineurin as a multifunctional regulator.
765 *J. Biochem.* **131,** 1–15 (2002).
766 45. Omar, M. H. & Scott, J. D. AKAP signaling islands: venues for precision
767 pharmacology. *Trends Pharmacol. Sci.* **41,** 933–946 (2020).
768 46. Gowers, D. M. & Halford, S. E. Protein motion from non-specific to specific
769 DNA by three-dimensional routes aided by supercoiling. *EMBO J.* **22,** 1410–
770 1418 (2003).
771 47. Vuzman, D., Azia, A. & Levy, Y. Searching DNA via a 'monkey bar' mechanism:
772 the significance of disordered tails. *J. Mol. Biol.* **396,** 674–684 (2010).
773 48. Levchenko, A. Allovalency: a case of molecular entanglement. *Curr. Biol.* **13,**
774 876–878 (2003).
775 49. Mondragon, A., Griffith, E. C., Sun, L., Xiong, F., Armstrong, C. & Liu, J. O.
776 Overexpression and purification of human calcineurin α from Escherichia coli
777 and assessment of catalytic functions of residues surrounding the binuclear
778 metal center. *Biochemistry* **36,** 4934–4942 (1997).
779 50. Jeong, J. Y., Yim, H. S., Ryu, J. Y., Lee, H. S., Lee, J. H., Seen, D. S. & Kang, S. G.
780 One-step sequence-and ligation-independent cloning as a rapid and versatile
781 cloning method for functional genomics Studies. *Appl. Environ. Microbiol.* **78,**
782 5440–5443 (2012).
783 51. Anthis, N. J. & Clore, G. M. Sequence-specific determination of protein and
784 peptide concentrations by absorbance at 205 nm. *Protein Sci.* **22,** 851–858
785 (2013).
786 52. Cavanagh, J., Skelton, N. J., Fairbrother, W. J., Rance, M. & Palmer, A. G. I.
787 *Protein NMR Spectroscopy Principles and Practice*. (Academic Press, 2006).
788 53. Panchal, S. C., Bhavesh, N. S. & Hosur, R. V. Improved 3D triple resonance
789 experiments , HNN and HN(C)N, for HN and 15N sequential correlations in

(13C,15N) labeled proteins : Application to unfolded proteins. *J. Biomol. NMR* **20,** 135–147 (2001).

54. Hyberts, S. G., Takeuchi, K. & Wagner, G. Poisson-gap sampling and forward maximum entropy reconstruction for enhancing the resolution and sensitivity of protein NMR data. *J. Am. Chem. Soc.* **132,** 2145–2147 (2010).

55. Bostock, M. J., Holland, D. J. & Nietlispach, D. Compressed sensing reconstruction of undersampled 3D NOESY spectra: Application to large membrane proteins. *J. Biomol. NMR* **54,** 15–32 (2012).

56. Vranken, W. F., Boucher, W., Stevens, T. J., Fogh, R. H., Pajon, A., Llinas, M., Ulrich, E. L., Markley, J. L., Ionides, J. & Laue, E. D. The CCPN data model for NMR spectroscopy: Development of a software pipeline. *Proteins Struct. Funct. Genet.* **59,** 687–696 (2005).

57. Farrow, N. A., Muhandiram, R., Singer, A. U., Pascal, S. M., Kay, C. M., Gish, G., Shoelson, S. E., Pawson, T., Forman-Kay, J. D. & Kay, L. E. Backbone dynamics of a free and a phosphopeptide-complexed Src homology 2 domain studied by ^{15}N NMR relaxation. *Biochemistry* **33,** 5984–6003 (1994).

58. Schuck, P. Size-distribution analysis of macromolecules by sedimentation velocity ultracentrifugation and Lamm equation modeling. *Biophys. J.* **78,** 1606–1619 (2000).

59. Laue, T. M., Shah, B. D., Ridgeway, T. M. & Pelletier, S. L. Computer-aided interpretation of analytical sedimentation data for proteins. *Anal. ultracentrifugation Biochem. Polym. Sci.* 90–125 (1992). doi:10.1006/abio.1995.1030